

Fault-segment rupture, aftershock-zone fluid flow, and mineralization

Steven Micklethwaite Research School of Earth Sciences, Australian National University, Canberra ACT 0200, Australia
Stephen F. Cox Research School of Earth Sciences, Australian National University, Canberra ACT 0200, Australia, and
Department of Earth and Marine Sciences, Australian National University, Canberra ACT 0200, Australia

ABSTRACT

We propose that zones of transient high permeability around ancient fault systems can be predicted if fault segments and likely locations for paleo-rupture arrest are identified. Lode gold deposits in the Kalgoorlie terrane, Western Australia, are the products of focused fluid flow through faulted crust. Deposits in the Mount Pleasant area are clustered on small-displacement structures over ~10 km of the >50-km-long Black Flag fault. Field relationships and net slip distribution along the fault indicate that the deposits are adjacent to, but not within, a kilometer-scale dilatant jog, where two segments of the fault are linked. On this basis we infer that the dilatant jog was a long-term rupture-arrest site. The observations are compatible with rupture on segments of the Black Flag fault changing stress in the surrounding crust and bringing specific zones closer to failure. By analogy with active seismogenic fault systems, those zones correspond to regions where aftershocks occur preferentially after failure. Stress-transfer modeling of the system helps explain the location of mineralized small-displacement structures around the Black Flag fault and indicates that gold deposits in the area are located on structures that became transiently permeable and localized fluid flow during repeated aftershock ruptures. Thus, localized through-flow, or mixing of fluids within fault systems, is likely to be controlled by the distribution of aftershocks following rupture events; this distribution is predictable.

Keywords: fault zones, aftershocks, fluids, mineral deposits, genesis, permeability, segmentation.

INTRODUCTION

In this paper we explain and predict a link between the nonuniform distribution of aftershocks around earthquakes and the evidence for nonuniform permeability around ancient fault systems. When an earthquake occurs on a fault, the rock volume around the rupture undergoes changes in stress state. Those volumes that are brought nearer to failure are closely associated with aftershocks (Harris, 1998, and references therein). Whether a volume is brought closer to failure can be estimated through stress-transfer modeling (Stein et al., 1992). In this way the distribution of aftershocks around seismogenic fault ruptures has been successfully modeled on a number of fault systems (King et al., 1994; Toda et al., 1998; Kilb and Rubin, 2002). In the Archean Kalgoorlie terrane, Western Australia, lode gold deposits are the products of fluid flow through faulted crust and are located within large fault systems (Eisenlohr et al., 1989). Gold deposits tend to occur on low-displacement structures around higher-displacement faults and shear zones (Eisenlohr et al., 1989). The deposits are often clustered along restricted parts of the crustal-scale shear network, and although commonly associated with certain rock types, deposits are found in a range of host rocks (Witt, 1993). Observations elsewhere in the world on fault-vein architecture and fluid-inclusion pressure variations have led several authors to suggest that similar low-displacement structures hosted aftershock ruptures (e.g., Robert et al., 1995; Henderson and McCaig, 1996; Cox et al., 2001). Cox and Ruming (2004) tested this hypothesis by applying stress-transfer modeling to explain deposit dis-

tribution around a large contractional fault jog at the St. Ives gold field, Western Australia.

In this study we apply stress-transfer modeling to the Mount Pleasant gold field in the Kalgoorlie terrane, where geological mapping and high-resolution aeromagnetic data provide good constraints on the associated Black Flag fault. This work advances from Cox and Ruming (2004) by using along-fault slip distribution and field observations to clearly identify ancient fault segmentation. We demonstrate that through the control of segmentation on rupture arrest sites and thus aftershocks, distinct zones of elevated permeability can develop repeatedly. Herein we propose a new conceptual model for seismogenic faulting and time-dependant fluid flow. We show that stress-transfer modeling has wider application than earthquake risk, with potential as a tool for mineral exploration.

FAULT GEOMETRY, SEGMENTATION, AND MINERALIZATION

The Black Flag fault is >50 km long. It crosscuts the Boorara and Zuleika shear zones near its northern and southern tips, respectively (Fig. 1A). At Mount Pleasant, a large zone of quartz veins and breccias marks a jog that deviates 22°E from the overall trend of the fault. Historically, some small deposits have been mined directly on the jog, but most deposits occur in subsidiary structures and splay off the main fault. From the jog zone to the north, the fault is hosted predominantly in units of mafic composition, i.e., the Mount Pleasant

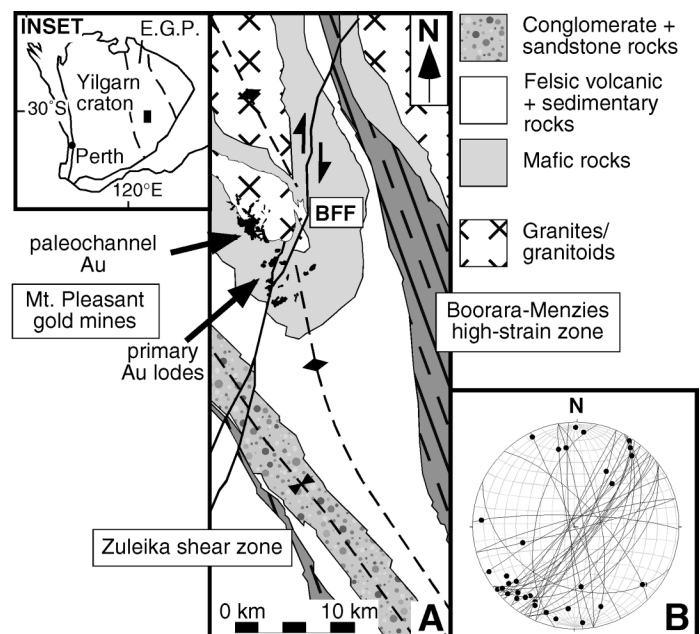


Figure 1. A: Geologic map of dextral Black Flag fault (BFF) and Mount Pleasant gold camp, Kalgoorlie terrane. Location shown by filled rectangle in inset. E.G.P.—Eastern Goldfields province. B: Stereoplot illustrating orientations of faults, shears, and shear-zone foliations from Black Flag fault. Lineations are stretching lineations and slickenlines. Kinematic indicators imply predominantly strike-slip movement.

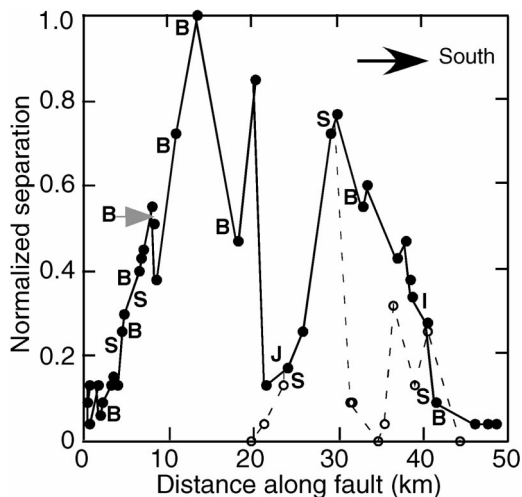


Figure 2. Fault strike separation vs. length profile for Black Flag fault. Geometrical features located along fault are indicated relative to profile; B—bend, I—fault intersection, J—jog, S—splay. Dashed lines represent data from large splays along fault.

dolerite sill plus the Bent Tree and Victorious basalt units. South of the jog, the majority of wall rock is felsic to intermediate lava, tuff, felsic volcanoclastic rocks, and sedimentary rocks of the Black Flag and White Flag Formations. A cluster of gold deposits occurs at Mount Pleasant as both primary lodes and paleochannel deposits derived from lodes (Fig. 1A). Primary lodes are found in a range of host rocks.

The large Black Flag fault is a dextral strike-slip fault with negligible oblique-slip components (Fig. 1B). A good constraint on strike separation (a proxy for displacement) is possible because of the number of lithologic intersections along strike. Strike separation along the fault varies by ~0.1–2.4 km. The resulting separation-length profile is marked by two large maxima and one large central minimum; second-order maxima and minima are superimposed over this pattern (Fig. 2). These minima are spatially associated with geometrical features like bends and splays, and the first-order central minimum is located at the fault's jog. In the field, the jog is a remarkable zone of dilation, up to 40 m wide and 2 km long. Through the jog zone the fault has 400 m of displacement across it and is a thin, cataclasite-rich fault plane (0.5–2 m thick). It is associated with a large number of subparallel, near-vertical, continuous quartz veins, plus silicified breccias containing both wall rock and preexisting vein fill. Many veins are massive or contain extension fibers, but there are also crustiform textures. In contrast, adjacent faults throughout the Mount Pleasant gold field are small and generally show dextral slip (Gebre-Mariam et al., 1993); some of them are associated with breccias, and they have displacements up to tens of meters. Associated veins are massive or laminated and rarely >1 m thick. Common vein-fault geometries indicate that σ_1 , during shearing, was subhorizontal with an azimuth of 060°. Veins also have alteration haloes marked by sericitization and carbonatization. This hydrothermal alteration overprints low-greenschist metamorphic assemblages, but metamorphism and metasomatism are broadly contemporary (e.g., Gebre-Mariam et al., 1993).

Taken together, these observations are attributed to the Black Flag fault being composed of two segments on the broad scale, highlighted by (1) a jog, (2) marked dilation, and (3) a minimum in cumulative displacement (cf. Peacock, 1991). The segments underlap north and south of the jog, respectively. For the majority of seismic events, the segments would have been mechanically separate, and the jog zone would have therefore constituted a common site for rupture termination, dilation, and enhanced fluid flow (Sibson, 1987). Structures ad-

acent to the jog are relatively immature, low-displacement fault and vein networks, which have acted as localized channels for high-flux fluid flow. Fluid-inclusion data have shown that deformation and mineralization occurred at ~250 °C, within the top 10 km of crust (Cassidy and Bennett, 1993; Gebre-Mariam et al., 1993). These simple observations provide excellent constraint for key parameters in the following modeling.

SEGMENT RUPTURE OF THE BLACK FLAG FAULT

We used a three-dimensional elastic half-space boundary element model (COULOMB 2.2.1) to calculate the change in Coulomb failure stress in crust immediately after a large rupture. Because positive changes in Coulomb failure stress have been shown to correlate well with zones of aftershocks, we use the Coulomb software to infer the distribution of aftershocks around ancient faults, when ruptured by large earthquakes. The approach was detailed in Stein et al. (1992), King et al. (1994), and Toda et al. (1998). Though we model ruptures of a given size, we are principally testing whether a range of ruptures commonly terminating at the fault's jog can explain the distribution of mineralization. The change in Coulomb failure stress ($\Delta\sigma_F$) gauges the proximity to failure of faults due to static changes in shear stress ($\Delta\tau$) and normal stress ($\Delta\sigma_n$). Here, using seismological convention,

$$\Delta\sigma_F = \Delta\tau + \mu'(\Delta\sigma_n), \quad (1)$$

where μ' is the apparent coefficient of friction. In equation 1, μ' encompasses the more familiar static coefficient of friction (μ) and the pore-pressure change because it is assumed that during rupture, stress changes much more rapidly than fluid pressure. In this scenario $\mu' = \mu(1 - B)$, where B is Skempton's coefficient (commonly $0.6 \leq B \leq 1$; Green and Wang, 1986). For crustal rocks B is not well understood, and several authors have suggested that low values of μ' may indicate high fluid pressures ($B \rightarrow 1$; e.g., Reasenberg and Simpson, 1992; Stein et al., 1992; Gross and Bürgmann, 1998). However, model results only change significantly at $\mu' < 0.1$, and $\mu' = 0.4$ is a reasonable value to use (King et al., 1994).

In the model, the Black Flag fault is represented by a vertical plane, with the present-day along-strike geometry and a depth range of 0–10 km. The $\Delta\sigma_F$ was sampled at 5 km, for optimally oriented planes. In this case, we allowed the large northern and southern segments, either side of the fault's jog, to rupture in separate models and under varying boundary conditions. Both segments are ~15 km long, which suggests that rupturing either full segment resulted in earthquakes with $M < 6.5$ (Kanamori and Anderson, 1975; Sibson, 1989; Wells and Coppersmith, 1994). By using empirical fault dimension vs. earthquake magnitude relationships, these values equate to 0.6 m dextral slip on the rupture planes.

We present the results in Figure 3, with the distribution of $\Delta\sigma_F$ from independent ruptures on the two segments summarized in Figure 3D. Our calculations show that the structures hosting gold mineralization correspond with the domains of positive $\Delta\sigma_F$, consistent with their being activated as aftershocks. In this scenario the predicted aftershock pattern and mineralization coincide not only in the region between underlapping fault segments, but also where lobes of positive stress are generated laterally (e.g., Fig. 3C). Further, the correlation of mineralization with the predicted aftershock pattern highlights the observation that these low-displacement aftershock structures are sites of more focused fluid flow relative to the main fault. We address this issue in the following conceptual model.

DISCUSSION AND CONCLUSIONS

In fault systems the most significant fluid migration is likely to take place during and after rupture events. At the fault-system scale, models based on fault architecture commonly identify jogs and bends

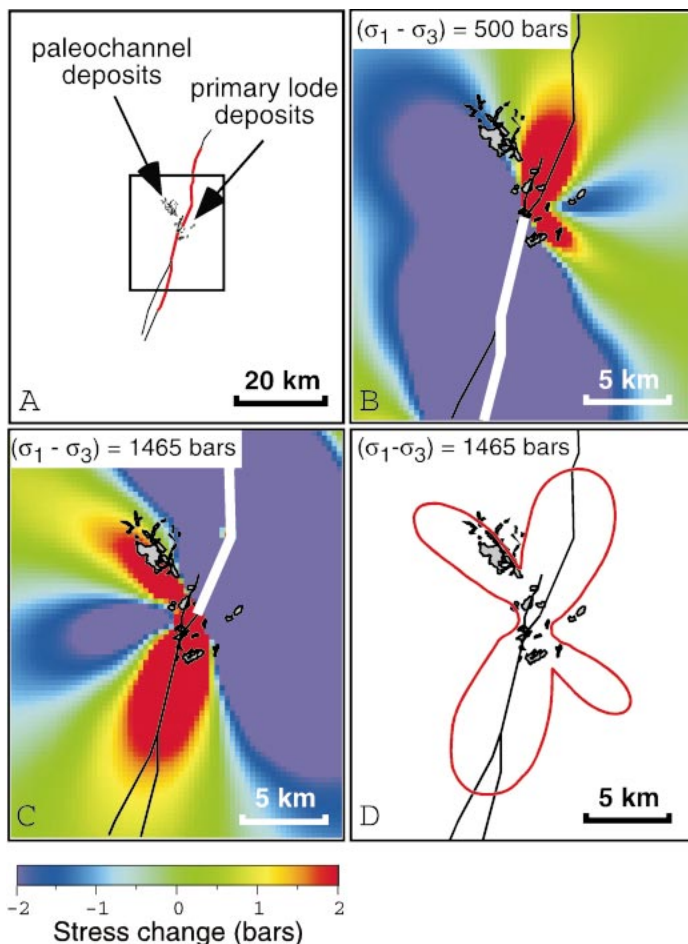


Figure 3. A: Model space with location of gold deposits relative to fault. Northern and southern segments ruptured in different models are highlighted in bold red and terminate at jog coincident with Mount Pleasant deposits. Elastic parameters varied dependent on main-segment host rock; northern segment $E = 8.0 \times 10^5$ bars, $\nu = 0.25$; southern segment $E = 5.0 \times 10^5$ bars, $\nu = 0.20$. Variations with differential stress ($\sigma_1 - \sigma_3$) were tested between models, with no change observed in $\Delta\sigma_F$ lobate pattern, or location, and only small effect on lobe size (e.g., compare size between B and C). Locations of images in B, C, and D are shown by rectangle in A. B and C: Example calculations of $\Delta\sigma_F$ for optimally oriented faults, predicting aftershock distribution that results from ruptures on southern (B) and northern (C) segments. D: Summary of predicted zone of aftershocks resulting from ruptures on Black Flag fault, which correlates with distribution of gold deposits. Contour of $\Delta\sigma_F = 1.5$ bars is shown in red.

as having a first-order control on permeability during rupture (Sibson, 1987). Nonetheless, if the Mount Pleasant gold camp is viewed as a marker of high fluid flux, then, although mineralization does occur on these sites, it is also localized up to 5 km away.

In the conceptual summary, presented in Figure 4, fluids flow up through the fault system. The same principles apply if the fault system is a site for mixing of different downwelling and upwelling fluids. We emphasize that during and shortly after rupture, both the ruptured fault zone and the aftershock zone are sites with enhanced permeability. However, more protracted fluid flow is likely to occur in the aftershock zones. Aftershock activity occurs over extended periods (months to decades for main shocks with $M > 6$), potentially maintaining a high-permeability network during that time. In contrast, on the main rupture surface, porosity is created over a broad area but is not maintained. Rapid sealing of the fluid pathways occurs by compaction and sealing of the damage products (e.g., Tenthorey et al., 2003). Therefore, rupture

on the main fault (time $t = 0$) leads to elevated fluid flux through the aftershock structures over a protracted period ($t = t_f$), but through the main structure for only a short period ($t \leq t_1$).

Using contemporary seismogenic fault systems as an analogue for understanding paleo-fault systems has led to a more robust understanding of fluid-flow localization. The results presented here argue that during seismic deformation on a fault system, the highest fluid flux is localized in sites determined by the location of aftershock networks (Fig. 4). Dilation at jogs and bends along the main shock fault does not matter so much as the fact that networks of faults undergoing aftershocks are located adjacent to such sites. Such networks arise because jogs and bends are sites for earthquake rupture arrest (Sibson, 1985; Wesnousky, 1988). Thus, contractional jogs or bends on large faults are just as likely to lead to transiently permeable zones of crust as a dilational jog (e.g., Cox and Ruming, 2004). We predict that crust between underlapping segments will be particularly subject to the highest fluid fluxes. Equally, the distribution of aftershocks can be not only between interacting fault segments, but also where lobes of positive $\Delta\sigma_F$ values are generated laterally.

This study has particular relevance for gold mineralization models in the Archean greenstone sequence of the Yilgarn craton. Different mineralization models have been proposed that all require fluid flow along faults (e.g. Groves, 1993; Witt et al., 1997), but the details of the fault-plumbing system remain unconstrained. The conceptual model presented resolves the disparity between clusters of well-mineralized small-displacement faults adjacent to poorly mineralized major faults, without necessitating physicochemical gradients between major and minor faults or different faults tapping different fluids (Eisenlohr et al., 1989). The distribution of areas of high permeability can be predicted with knowledge of the fault segmentation and of how stresses were transferred around appropriate ruptures.

ACKNOWLEDGMENTS

This work was supported by an Australian Research Council Linkage and Australian Mineral Industry Research Association grant. We thank Placerdome Ltd. for financial and logistical support, including access to mine sites and company data. Our research with Placerdome Ltd. was aided by discussions and field work with G. Tripp, P. Smith, R. Henderson, B. Davis, and M. Coutts. We also thank the U.S. Geological Survey and S. Toda for making the Coulomb modeling package freely available, and S. Gross and J. Evans for constructive and encouraging reviews.

REFERENCES CITED

- Cassidy, K.F., and Bennett, J.M., 1993, Gold mineralisation at the Lady Bountiful Mine, Western Australia: An example of a granitoid-hosted Archean lode gold deposit: *Mineralium Deposita*, v. 28, p. 388–408.
- Cox, S.F., and Ruming, K., 2004, The St. Ives mesothermal gold system, Western Australia—A case of golden aftershocks?: *Journal of Structural Geology*, v. 26, p. 1109–1125.
- Cox, S.F., Knackstedt, M.A., and Braun, J., 2001, Principles of structural control on permeability and fluid flow in hydrothermal systems: *Reviews in Economic Geology*, v. 14, p. 1–24.
- Eisenlohr, B.N., Groves, D., and Partington, G.A., 1989, Crustal-scale shear zones and their significance to Archean gold mineralization in Western Australia: *Mineralium Deposita*, v. 24, p. 1–8.
- Gebre-Mariam, M., Groves, D.I., McNaughton, N.J., Mikucki, E.J., and Vearncombe, J.R., 1993, Archean Au-Ag mineralisation at Racetrack, near Kalgoorlie, Western Australia: A high crustal-level expression of the Archean composite lode-gold system: *Mineralium Deposita*, v. 28, p. 375–387.
- Green, D.H., and Wang, H.F., 1986, Fluid pressure response to undrained compression in saturated sedimentary rocks: *Geophysics*, v. 51, p. 948–956.
- Gross, S., and Bürgmann, R., 1998, Rate and state of background stress estimated from the aftershocks of the 1989 Loma Prieta, California, earthquake: *Journal of Geophysical Research*, v. 103, p. 4915–4927.
- Groves, D.A., 1993, The crustal continuum model for late-Archean lode-gold deposits of the Yilgarn block, Western Australia: *Mineralium Deposita*, v. 28, p. 366–374.
- Harris, R.A., 1998, Introduction to special section: Stress triggers, stress shadows, and implications for seismic hazard: *Journal of Geophysical Research*, v. 103, p. 24,347–24,358.
- Henderson, I.H.C., and McCaig, A.M., 1996, Fluid pressure and salinity vari-

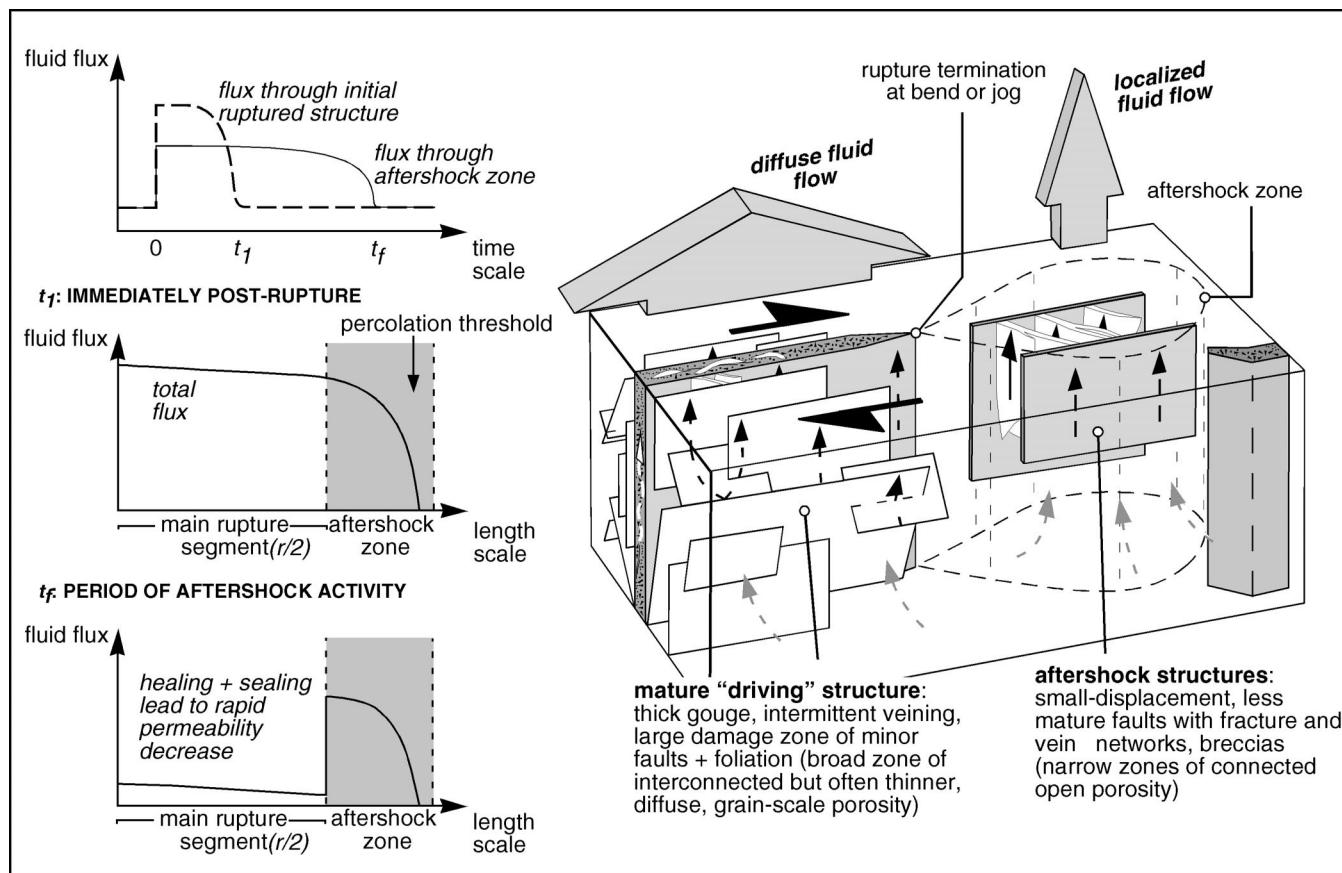


Figure 4. Conceptual model of fluid flow at jog in main structure; flow is due to rupture of main and aftershock structures. Aftershocks occur over protracted time period, maintaining high permeability relative to that of main rupture surface. Schematic profiles of fluid flux vs. time and fluid flux vs. fault length are inset; $r/2$ —half rupture segment length. Over repeated events, cumulative fluid flux will be greatly enhanced in aftershock zone.

- ations in shear zone-related veins, central Pyrenees, France: Implications for the fault-valve model: *Tectonophysics*, v. 262, p. 321–348.
- Kanamori, H., and Anderson, D.L., 1975, Theoretical basis of some empirical relations in seismology: *Seismological Society of America Bulletin*, v. 65, p. 1073–1095.
- Kilb, D., and Rubin, A.M., 2002, Implications of diverse fault orientations imaged in relocated aftershocks of the Mount Lewis, M_L 5.7, California, earthquake: *Journal of Geophysical Research*, v. 107, no. B11, doi: 10.1029/2001JB000149.
- King, G.C.P., Stein, R.S., and Lin, J., 1994, Static stress changes and the triggering of earthquakes: *Seismological Society of America Bulletin*, v. 84, p. 935–953.
- Peacock, D.C.P., 1991, Displacements and segment linkage in strike-slip fault zones: *Journal of Structural Geology*, v. 13, p. 1025–1035.
- Reasenber, P., and Simpson, R.W., 1992, Response of regional seismicity to the static stress change produced by the Loma Prieta earthquake: *Science*, v. 255, p. 1687–1690.
- Robert, F., Boullier, A.-M., and Firdaous, K., 1995, Gold-quartz veins in metamorphic terranes and their bearing on the role of fluids in faulting: *Journal of Geophysical Research*, v. 100, p. 12,861–12,881.
- Sibson, R.H., 1985, Stopping of earthquake ruptures at dilational fault jogs: *Nature*, v. 316, p. 248–250.
- Sibson, R.H., 1987, Earthquake rupturing as a mineralizing agent in hydrothermal systems: *Geology*, v. 15, p. 701–704.
- Sibson, R.H., 1989, Earthquake faulting as a structural process: *Journal of Structural Geology*, v. 11, p. 1–14.
- Stein, R.S., King, G.C.P., and Lin, J., 1992, Change in failure stress on the southern San Andreas fault system caused by the 1992 magnitude = 7.4 Landers earthquake: *Science*, v. 258, p. 1328–1331.
- Tenthorey, E., Cox, S.F., and Todd, H.F., 2003, Evolution of strength recovery and permeability during fluid-rock reaction in experimental fault zones: *Earth and Planetary Science Letters*, v. 206, p. 161–172.
- Toda, S., Stein, R.S., Reasenber, P.A., Dieterich, J.H., and Yoshida, A., 1998, Stress transferred by the 1995 $M_W = 6.9$ Kobe, Japan, shock: Effect on aftershocks and future earthquake probabilities: *Journal of Geophysical Research*, v. 103, p. 24,543–24,565.
- Wells, D.L., and Coppersmith, K.J., 1994, New empirical relationships among magnitude, rupture length, rupture width, rupture area, and surface displacement: *Seismological Society of America Bulletin*, v. 84, p. 974–1002.
- Wesnousky, S.G., 1988, Seismological and structural evolution of strike-slip faults: *Nature*, v. 335, p. 340–343.
- Witt, W.K., 1993, Lithological and structural controls on gold mineralisation in the Archean Menzies-Kambalda area, Western Australia: *Australian Journal of Earth Sciences*, v. 40, p. 65–80.
- Witt, W.K., Knight, J.T., and Mikucki, E.J., 1997, A synmetamorphic lateral fluid flow model for gold mineralization in the Archean southern Kalgoorlie and Norseman terranes, Western Australia: *Economic Geology*, v. 92, p. 407–437.
- Manuscript received 10 February 2004
 Revised manuscript received 14 May 2004
 Manuscript accepted 18 May 2004
- Printed in USA